A Covariance Analysis Tool for Assessing Fundamental Limits of SIM Pointing Performance

David S. Bayard and Bryan H. Kang

Jet Propulsion Laboratory, California Institute of Technology, Pasadena, CA, 91109, USA

ABSTRACT

This paper presents a performance analysis of the instrument pointing control system for NASA's Space Interferometer Mission (SIM). SIM has a complex pointing system that uses a fast steering mirror in combination with a multirate control architecture to blend feedforward information with feedback information. A pointing covariance analysis tool (PCAT) is developed specifically to analyze systems with such complexity. The development of PCAT as a mathematical tool for covariance analysis is outlined in the paper. PCAT is then applied to studying performance of SIM's science pointing system. The analysis reveals and clearly delineates a fundamental limit that exists for SIM pointing performance. The limit is especially stringent for dim star targets. Discussion of the nature of the performance limit is provided, and methods are suggested to potentially improve pointing performance.

Keywords: pointing control, covariance analysis, fast steering mirrors, fundamental performance limits

1. INTRODUCTION

NASA's Space Interferometer Mission (SIM) uses interferometric-based astrometry to detect and characterize Earth-like planetary systems around neighboring stars, and provide observations that help answer fundamental astrophysics questions about galaxies and the origins of the universe[5,6] A critical element of the SIM instrument is the capability to perform stable and accurate angle tracking of stars that are used for fringe generation inside the instrument. An overview of the SIM real-time control system architecture is given in Kang et. al.[4] Fast-steering mirror (FSM) control is used for pointing the SIM camera, and to effectively direct light down a precise path into the interferometer. The FSM control architecture is composed of both feedback and feedforward loops. The role of the feedforward loop, in particular, is to use extra information available from a separate guide camera, to improve dim-star pointing for which closed-loop feedback is severely limited by long camera exposures.

A pointing covariance analysis tool, PCAT, has been specifically designed to analyze SIM's complex architecture and study basic trade-offs, characterize limits of performance, and assess overall pointing capability. Covariance analysis is useful because it numerically calculates RMS performance in a single run.[3] This can be contrasted with Monte Carlo analysis that typically requires thousands of runs to get an approximate answer to the same problem. PCAT has proved especially useful in SIM pointing studies by evaluating performance over a multitude of choices for star type, star magnitudes, and exposure times. The PCAT tool development is discussed in the paper, drawing necessary results from linear system theory, covariance analysis, matrix theory, and spectral analysis. Tool development includes careful modeling of the finite camera exposure using linear system elements, as well as rigorous treatment of the SIM multirate control architecture. The PCAT framework is specialized to analyzing SIM science pointing performance, giving rise to PCAT-S.

PCAT is then applied to studying performance of the SIM science pointing system. The analysis reveals and clearly delineates a fundamental limit that exists on SIM pointing performance. This limit arises from trying to optimally balance the effects of process noise (thermal drift) that worsens for long exposures, with measurement noise (camera centroiding errors) that worsens for short exposures. These effects are balanced through the determination of an optimal exposure time, computed as a function of star magnitude and type. The resulting analysis clearly indicates fundamental trade-offs and difficulties inherent to dim star pointing. Results of the covariance analysis are summarized in terms of a family of optimal designs, corresponding to best exposure times and best attainable RMS pointing performance. The nature of the fundamental pointing performance limit is discussed. Results in this paper are drawn from an earlier JPL document.[2]

2. COVARIANCE ANALYSIS FRAMEWORK

The idea behind covariance analysis is to propagate the system covariance rather than the system trajectories. In this way, a single run of a covariance analysis can provide the same information about RMS performance as many thousands of Monte Carlo simulation runs. The layout used for PCAT-based covariance analysis is the generic pointing system shown in Figure 2.1. The pointing system is comprised of a system having two time scales - a slow scale and a fast scale. The slow scale is associated with a digital control loop that is wrapped around the entire system. The sampling rate for the slow scale is determined by camera exposure times, since this dictates the rate at which centroid measurements become available to the digital controller for use in determining the feedback control. The fast scale contains everything else in the loop, and is modeled in its largest part by the Generic Plant (GP) model shown in Figure 2.1. The GP model can be chosen differently depending on the intended application. Generally, the GP model includes the plant dynamics, actuator dynamics including any inner-loop controllers wrapped around the actuators and operating at higher bandwidths, the contribution of various physical noise sources and load disturbances, as well as signal generation of disturbance estimates that are used for feedforward compensation. The quantity z in Figure 2.1 is the main pointing signal. It is desired for z to track the reference r through the use of feedback from camera centroid measurements, and possibly additional feedforward signals that approximate disturbances entering the system at various locations. Augmenting the GP model with the camera delay and camera integrator state, gives the Augmented Generic Plant (AGP) model shown in Figure 2.1.

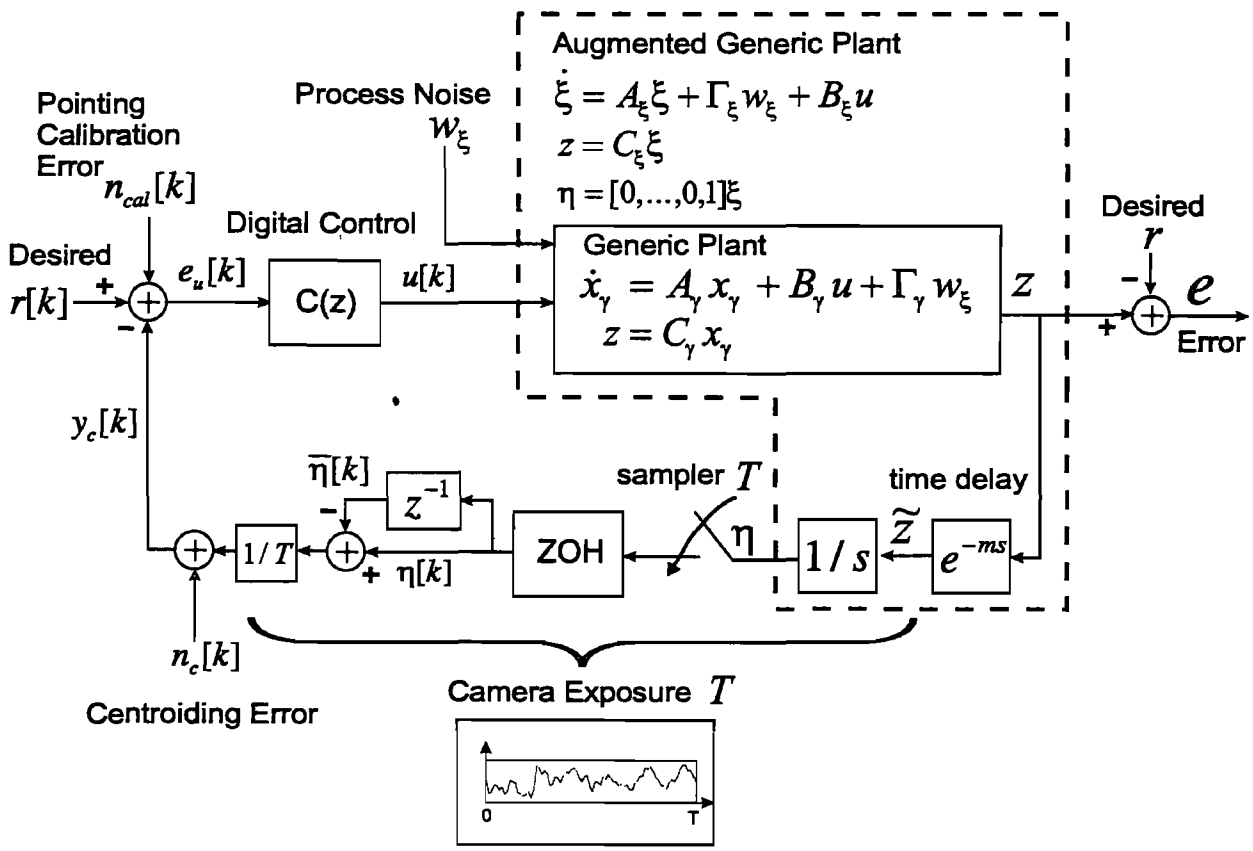

Figure 2.1. Generic framework for pointing covariance analysis.

2.1 Generic Plant (GP) Model

A generic plant (GP) model $A_\gamma, B_\gamma, \Gamma_\gamma, C_\gamma$ is defined that the user can modify arbitrarily to model various pointing system architectures of interest,

$$\dot{x}_\gamma = A_\gamma x_\gamma + B_\gamma u + \Gamma_\gamma w_\xi \tag{2.1}$$

$$z = C_\gamma x_\gamma \tag{2.2}$$

The GP model is constructed to take the controller command u and an arbitrary process noise vector w_ξ as inputs, and to provide the desired pointing signal z as output.

By choosing the GP model differently, the PCAT tool can be applied to any control system that makes use of camera-based feedback. This GP model will be made specific later in the paper to define PCAT-S for the SIM science pointing subsystem. It has also been applied to defining PCAT-G for the SIM guide pointing subsytem, discussed elsewhere.[2] The reader can modify the GP model appropriately to apply the PCAT formalism to his or her own application.

2.2 Camera System Delay Models

A Pade approximation is used to model a delay of m seconds associated with latencies in the camera system (processing-delay only, not including the camera exposure time which is captured elsewhere), plus additional data acquisition and processing times.

$$\dot{x}_m = A_m x_m + B_m u_m \tag{2.3}$$

$$\tilde{z} = C_m x_m + D_m u_m \tag{2.4}$$

This delay model takes the pointing process $u_m = z$ as input, and produces a delayed pointing process $\tilde{z}$ as output. Physically, this delay often comes *after* the camera exposure in the block diagram. However, since the system is linear, there is no error incurred in modeling it *before* to camera exposure, where it has the advantage of being simply represented by a rational (Pade) approximation.

2.3 Camera Integrator State

In order to properly model the finite-time camera exposure, an integrator is added after the time delay (cf., Figure 2.1). The integrator acts on $\tilde{z}$ to model the effect of photon accumulation within the camera's detector.

$$\dot{\eta} = \tilde{z} \tag{2.5}$$

The camera integrator takes the delayed pointing process $\tilde{z}$ as input, and produces the integrated quantity η as output.

2.4 Augmented Generic Plant (AGP) Model

An Augmented Generic Plant (AGP) model is defined by augmenting the GP model (2.1)(2.2), with the camera delay (2.3)(2.4) and the integrator state (2.5),

$$\begin{bmatrix} \dot{x}_\gamma \\ \dot{x}_m \\ \dot{\eta} \end{bmatrix} = \begin{bmatrix} A_\gamma & O & O \\ B_m C_\gamma & A_m & O \\ D_m C_\gamma & C_m & O \end{bmatrix} \begin{bmatrix} x_\gamma \\ x_m \\ \eta \end{bmatrix} + \begin{bmatrix} \Gamma_\gamma \\ O \\ O \end{bmatrix} w_\xi + \begin{bmatrix} B_\gamma \\ O \\ O \end{bmatrix} u \tag{2.6}$$

Here, the symbol O is used to denote a matrix of all zeros having appropriate compatible dimensions. The system (2.6) can be associated with the augmented state vector,

$$\xi \triangleq \begin{bmatrix} x_\gamma \\ x_m \\ \eta \end{bmatrix} \tag{2.7}$$

The resulting state-space model with measurements can be written in terms of ξ as,

$$\dot{\xi} = A_\xi \xi + B_\xi u + \Gamma_\xi w_\xi \tag{2.8}$$

$$z = C_\xi \xi = [C_\gamma, O\,, O\,]\xi \tag{2.9}$$

$$\tilde{z} = \tilde{C}_\xi \xi = [D_m C_\gamma, C_m, O\,]\xi \tag{2.10}$$

$$\eta = [O\,, O\,, 1]\xi \tag{2.11}$$

For later use, it will be convenient to define a shortened version of ξ, denoted as ξ_s, that does not include its last scalar element η, i.e.,

$$\xi = \begin{bmatrix} \xi_s \\ \eta \end{bmatrix}; \quad \xi_s \triangleq \begin{bmatrix} x_\gamma \\ x_m \end{bmatrix} \tag{2.12}$$

2.5 Camera Exposure Model

The camera exposure of duration T is modeled using linear system elements as shown in Figure 2.1. Specifically, a centroid measurement $y_c[k]$ at time $t = kT$ can be written as,

$$\begin{aligned} y_c[k] &\triangleq \frac{1}{T}\left(\int_{(k-1)T}^{kT} \tilde{z}(t)dt\right) + n_c[k] \\ &= \frac{1}{T}\left(\int_0^{kT} \tilde{z}(t)dt - \int_0^{(k-1)T} \tilde{z}(t)dt\right) + n_c[k] \\ &= \frac{1}{T}\Big(\eta(kT) - \eta((k-1)T)\Big) + n_c[k] \\ &= \frac{1}{T}\Big(\eta[k] - \eta[(k-1]\Big) + n_c[k] \end{aligned} \tag{2.13}$$

where the bracket notation $x[k]$ is used to denote the digitization of a continuous-time quantity $x(t)$ at discrete-time instant $t = kT$. The digital noise term $n_c[k]$ denotes a zero-mean discrete-time centroiding error with covariance,

$$\sigma_c^2(k) = Cov(n_c[k]) \tag{2.14}$$

Let $\overline{\eta}[k]$ be a delayed version of $\eta[k]$,

$$\overline{\eta}[k] \triangleq \eta[k-1] \tag{2.15}$$

Substituting (2.15) into (2.13) gives the desired expression for the centroid measurement,

$$y_c[k] = \frac{1}{T}\left(\eta[k] - \overline{\eta}[k]\right) + n_c[k] \tag{2.16}$$

2.6 Digital Controller

A digital controller with state x_u is specified in state-space form as,

$$x_u[k+1] = A_u x_u[k] + B_u e_u[k] \tag{2.17}$$

$$u[k] = C_u x_u[k] \tag{2.18}$$

The commanded position is denoted as $r[k]^o$ where,

$$r^o[k] = r[k] + n_{cal}[k] \tag{2.19}$$

The quantity $n_{cal}[k]$ is the difference between the ideal reference command $r[k]$ and the commanded value $r^o[k]$ that occurs due to imperfect pointing calibration. It is modeled as white noise with covariance,

$$\sigma_{cal}^2 = Cov(n_{cal}[k]) \tag{2.20}$$

The error $e_u[k]$ that drives the digital controller is the difference between the commanded reference location $r^o[k]$ and the last held centroid measurement $y_c[k]$, i.e.,

$$e_u[k] = r^o[k] - y_c[k] \tag{2.21}$$

Substituting (2.16) and (2.19) into (2.21) gives upon rearranging,

$$e_u[k] = r[k] - \frac{1}{T}\left(\eta[k] - \overline{\eta}[k]\right) + n_{cal}[k] - n_c[k] \tag{2.22}$$

Without loss of generality for covariance analysis, the constant reference is taken as $r[k] \equiv 0$. Substituting (2.22) into (2.17) gives upon rearranging,

$$x_u[k+1] = A_u x_u[k] - \frac{1}{T} B_u\ \eta[k] + \frac{1}{T} B_u\ \overline{\eta}[k] + B_u(n_{cal}[k] - n_c[k]) \tag{2.23}$$

This provides the discrete-time propagation of the digital controller state $x_u[k]$.

3. COVARIANCE PROPAGATION

3.1 Full State Definition

The full state vector x is formed by augmenting ξ with digital states x_u and $\overline{\eta}$ to give,

$$x \triangleq \begin{bmatrix} x_u \\ \xi \\ \overline{\eta} \end{bmatrix} \tag{3.1}$$

Let the covariance of x be denoted by P,

$$P \triangleq Cov(x) \tag{3.2}$$

The covariance must be propagated through both open-loop and closed-loop stages. This process is depicted in Figure 3.1, aided by a special notation that is now discussed. Time in seconds is written in double-index notation $t = [k, \tau]$ which has the meaning,

$$t = (k-1)T + \tau \triangleq [k, \tau] \tag{3.3}$$

Here T is the camera exposure time; k is an integer denoting the index of the camera exposure; and τ denotes the time (in seconds), that has passed relative to the start of the current exposure. The quantity τ is constrained as $\tau \in [0, T]$. The double-index notation is convenient because, as shown in Figure 3.1, the system propagates open-loop as a continuous function of time τ *during* each camera exposure, and in closed-loop at the discrete instants of time k at *completion* of each exposure.

3.2 Continuous-Time (CT) Propagation Model

During open-loop propagation, the controller, the augmented generic plant model, and camera states are connected to give the following state equations,

$$\begin{bmatrix} \dot{x}_u \\ \hline \dot{\xi}_s \\ \dot{\eta} \\ \hline \dot{\overline{\eta}} \end{bmatrix} = \begin{bmatrix} O & [\ O \quad O\ ] & O \\ B_\xi C_u & A_\xi & O \\ O & [\ O \quad O\ ] & O \end{bmatrix} \begin{bmatrix} x_u \\ \hline \xi_s \\ \eta \\ \hline \overline{\eta} \end{bmatrix} + \begin{bmatrix} O \\ \hline \Gamma_\xi \\ \hline O \end{bmatrix} w_\xi \tag{3.4}$$

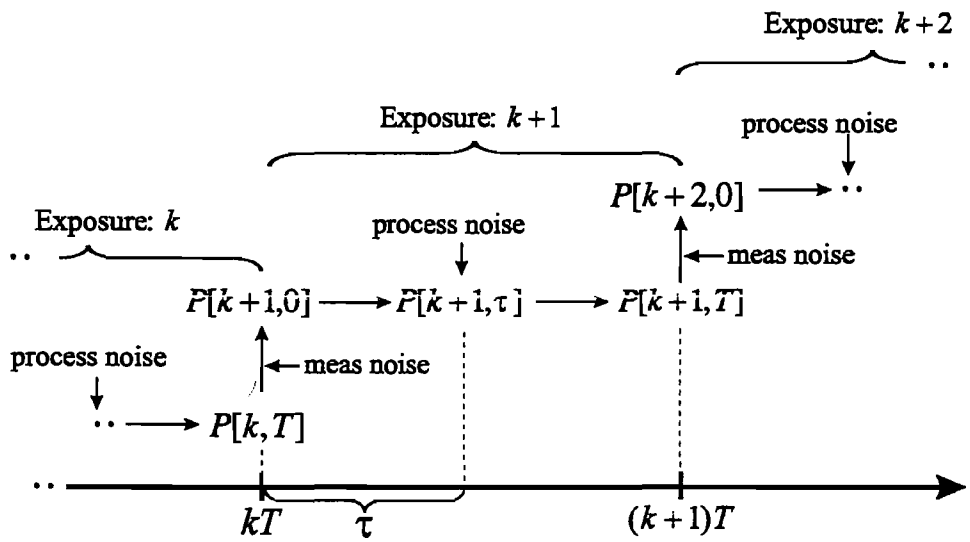

Figure 3.1. Timeline indicating successive camera exposures of duration T.

It is seen that the digital camera state $\overline{\eta}$ is held constant over each camera exposure, consistent with the hold-function seen in Figure 2.1. Likewise, the digital controller state x_u is held constant consistent with a computer-based digital controller implementation. The system equations (3.4) are equivalent to,

$$\dot{x}[k,\tau] = A_{CT}\, x[k,\tau] + \Gamma_{CT}\, w_{CT}(t) \tag{3.5}$$

where,

$$A_{CT} \triangleq \begin{bmatrix} O & [\,O \quad O\,] & O \\ B_\xi C_u & A_\xi & O \\ O & [\,O \quad O\,] & O \end{bmatrix}; \quad \Gamma_{CT} \triangleq \begin{bmatrix} O \\ \hline \Gamma_\xi \\ \hline O \end{bmatrix} \tag{3.6}$$

$$w_{CT}(t) \triangleq w_\xi \tag{3.7}$$

For later use, it is convenient to define a noise covariance matrix,

$$Q_{CT} = \Gamma_{CT}\, W_{CT}\, \Gamma_{CT}^T \tag{3.8}$$

where the CT noise $w_{CT}(t)$ is delta-correlated as,

$$E[w_{CT}(t+\tau) w_{CT}(t)^T] \triangleq W_{CT}\, \delta(\tau) \tag{3.9}$$

3.3 Discrete-Time (DT) Propagation Model

At the end of the $k+1$'th epoch when $t = (k+1)T$, a centroid measurement $y_c[k]$ becomes available and a DT update is made of the form,

$$\begin{bmatrix} x_u \\ \hline \xi_s \\ \eta \\ \hline \overline{\eta} \end{bmatrix}_{k+1} = \begin{bmatrix} A_u & [\,O \quad -\frac{1}{T}B_u\,] & \frac{1}{T}B_u \\ O & I & O \\ O & [\,O \quad I\,] & O \end{bmatrix} \begin{bmatrix} x_u \\ \hline \xi_s \\ \eta \\ \hline \overline{\eta} \end{bmatrix}_k + \begin{bmatrix} B_u \\ \hline O \\ \hline O \end{bmatrix} (n_{cal}[k] - n_c[k]) \tag{3.10}$$

Here, the centroid $y_c[k]$ from the camera exposure feeds into the controller using (2.23) via the top row of the state-space model. The bottom-most row shows the latching of the integral state η into $\overline{\eta}$, consistent with the sampling function shown in Figure 2.1. Equations (3.10) can be equivalently written as,

$$x[k+1,0] = A_{DT}\, x[k,T] + \Gamma_{DT}\, w_{DT}[k] \tag{3.11}$$

where,

$$A_{DT} \triangleq \begin{bmatrix} A_u & \begin{bmatrix} O & -\frac{1}{T}B_u \end{bmatrix} & \frac{1}{T}B_u \\ O & I & O \\ O & \begin{bmatrix} O & I \end{bmatrix} & O \end{bmatrix}, \quad \Gamma_{DT} \triangleq \begin{bmatrix} B_u \\ \hline O \\ \hline O \end{bmatrix} \tag{3.12}$$

$$w_{DT}[k] = n_{cal}[k] - n_c[k] \tag{3.13}$$

For later use, it is convenient to define a noise covariance matrix,

$$Q_{DT}[k] = Cov(\Gamma_{DT}\, w_{DT}[k]) = \Gamma_{DT}\, W_{DT}[k]\, \Gamma_{DT}^T \tag{3.14}$$

where,

$$W_{DT}[k] \triangleq Cov(w_{DT}[k]) \tag{3.15}$$

3.4 Covariance Propagation Computations

During the k'th camera exposure, the covariance P is propagated in continuous-time as,

$$\dot{P}[k,\tau] = A_{CT}P[k,\tau] + P[k,\tau]A_{CT}^T + Q_{CT}, \quad \tau \in [0,T] \tag{3.16}$$

where the CT state-space matrices (A_{CT}, Q_{CT}) are specified in (3.6). The value $\tau = 0$ always corresponds to the beginning of an exposure, and $\tau = T$ to the end of an exposure. At the end of the k'th exposure, the covariance is updated in discrete-time as,

$$P[k+1,0] = A_{DT}P[k,T] + P[k,T]A_{DT}^T + Q_{DT}[k] \tag{3.17}$$

where the DT state-space matrices (A_{DT}, Q_{DT}) are specified in (3.12). At the end of the discrete-time update, the next exposure begins, and the covariance is again propagated in continuous-time as,

$$\dot{P}[k+1,\tau] = A_{CT}P[k+1,\tau] + P[k+1,\tau]A_{CT}^T + Q_{CT}, \quad t \in [0,T] \tag{3.18}$$

This process is repeated for the duration of the run.

4. SCIENCE POINTING SYSTEM

For science pointing, the covariance analysis tool is arranged as shown in Figure 4.1. The main control loop is digital and runs at a sampling rate determined by the camera exposure duration T. When imaging dim stars, the exposures can be considerably longer than when imaging bright stars. For example, an exposure for a 19th magnitude star takes several hundred seconds, leading to a very slow digital control loop. The digital controller gains typically need to be scheduled based on the exposure time T. Multiple error sources are included as shown in Figure 4.1, comprised of pointing calibration error, science centroiding error, guide centroiding error, common and uncommon thermal drift, FSM quantization and mechanical error, ACS motions, and reaction wheel (RWA) induced jitter. Error models are discussed in more detail in Bayard and Kang.[2]

To partially offset the effects of long exposures, the science control loop uses an angle feedforward (AFF) signal $\widehat{d}$ that is available at the fast sampling rate. Physically, $\widehat{d}$ is a real-time estimate of the disturbance d entering the control loop at the point shown in Figure 4.1. The AFF signal $\widehat{d}$ is generated by a separate guide pointing system that centroids a bright star at a fast rate, and effectively tracks out disturbances that are strongly correlated to the science disturbances. If the plant were unity (i.e., $P(s) = 1$), and the AFF signal were

perfect (i.e., $\widehat{d} = d$), then a perfect rejection of disturbance d would occur. Unfortunately, the signal $\widehat{d}$ is only an estimate of d generated by measurements made every Δt seconds on a guide detector having centroiding error n_d with covariance σ_d^2. Furthermore, a time delay of duration ℓ seconds is incurred associated with the latency in communicating the AFF signal from the guide side of the instrument to the science side. A low-pass filter F_α is added to improve signal-to-noise characteristics of the AFF signal.

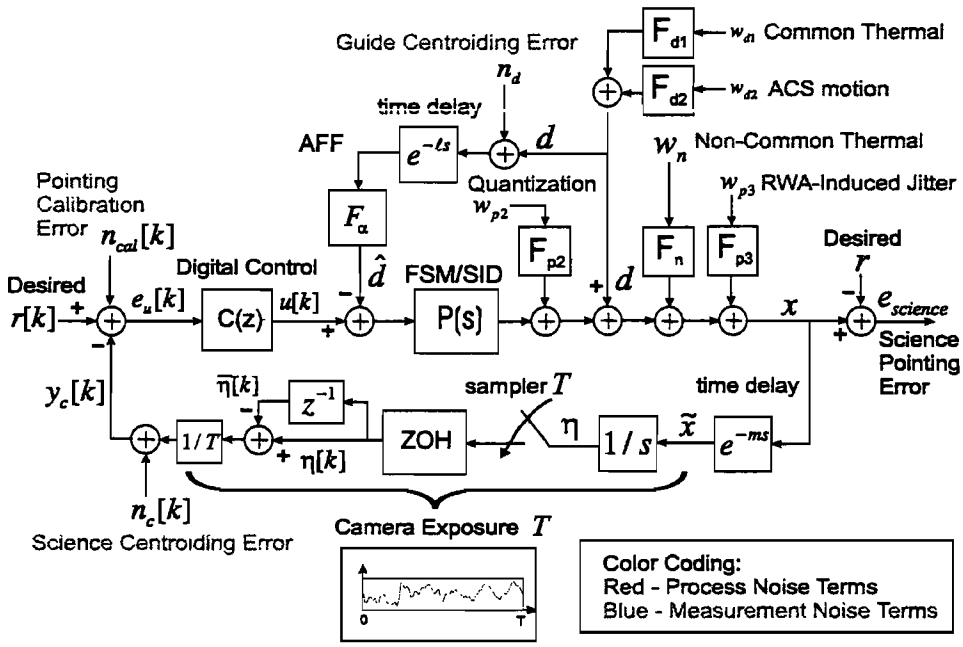

s

Figure 4.1. PCAT-S for covariance analysis of science pointing performance.

4.1 Science Pointing Performance Metric

The system depicted in Figure 4.1 is a special case of that shown in Figure 2.1, and as such, generates a full state vector x. Details are given in Bayard and Kang.[2] The covariance of x is denoted by P and is propagated by PCAT-S as,

$$P(t) \triangleq Cov[x(t)] \tag{4.1}$$

The main performance metric for the science pointing system is,

$$e_{science} \triangleq z - r = z = [O\,, C_\xi, O\,]x \triangleq C_{science}x \tag{4.2}$$

$$C_{science} \triangleq [O\,, C_\xi, O\,] \tag{4.3}$$

where we have used the fact that $r = 0$ by definition. The quantity $e_{science}$ is the science pointing error as a function of time. The desired RMS pointing error is extracted from the propagated covariance P as follows,

$$\sigma_{science}(t) = \sqrt{C_{science}P(t)C_{science}^T} \tag{4.4}$$

A typical plot of $\sigma_{science}(t)$ versus time is shown in Figure 4.2. The sawtooth character of the error arises from thermal drift that causes the covariance to grow during each exposure of duration T, and the centroid measurement that causes the covariance to collapse down to a smaller value after each exposure.

Because $\sigma_{science}(t)$ varies with time, it is convenient to define the *total* RMS pointing error based on an additional time average taken over period of T_{rms} seconds,

$$\sigma_{total} \triangleq \left(\frac{1}{T_{rms}}\int_0^{T_{rms}} \sigma_{science}^2(t)dt\right)^{\frac{1}{2}} \tag{4.5}$$

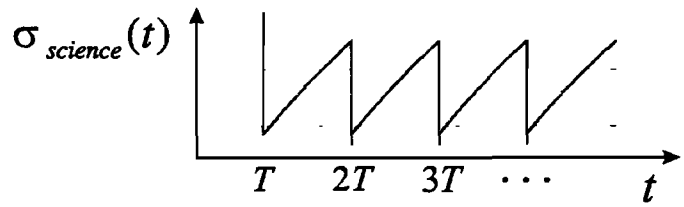

Figure 4.2. Typical result from PCAT-S for SIM science pointing analysis.

5. FUNDAMENTAL LIMITS OF SIM POINTING PERFORMANCE

In order to understand the fundamental limits of SIM pointing performance, the error budget is separated into three terms,

$$\sigma^2_{total}(T) = \sigma^2_c(T) + \sigma^2_n(T) + \sigma^2_{fixed} \tag{5.1}$$

where $\sigma_n(T)$ denotes the noncommon thermal drift, $\sigma_c(T)$ denotes the centroiding error associated with an exposure of time T, and σ^2_{fixed} denotes all other errors in the analysis that do not depend on the exposure time T. The noncommon thermal drift $\sigma_n(T)$ is the component of thermal drift physically local to the science pointing system and therefore is not cancelled by (i.e., is not common-mode with), the guide-generated feedforward signal. Since $\sigma_n(T)$ is time-varying, it is budgeted in the RMS sense (4.5) defined over each exposure period $T_{rms} = T$.

The three terms of (5.1) are summed up in a root-sum-square (RSS) fashion in Figure 5.1. Because $\sigma^2_n(T)$ increases with T while $\sigma^2_c(T)$ decreases with T, the sum results in a parabolic-like response that contains a natural minimum value. Conceptually, performance is limited for short exposures by large centroiding error (solid green line) but limited for long exposures by large noncommon thermal drift error (thick black line including fixed errors). Hence the total pointing error (dashed green) is minimized at the indicated exposure time. *This design point defines a fundamental limit beyond which the pointing performance cannot be improved.*

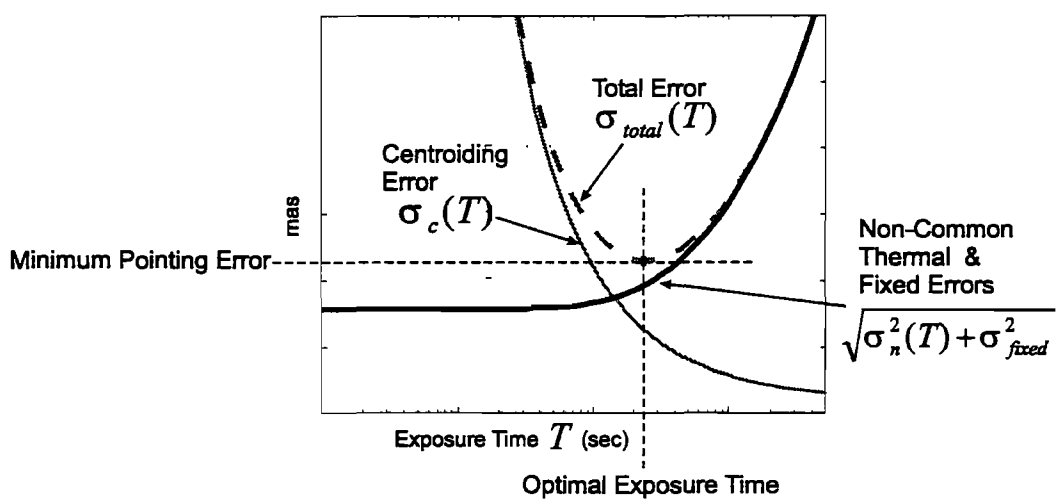

Figure 5.1. Total pointing error (dashed green line) versus exposure time (sec), showing optimal pointing design at minimum

6. SCIENCE POINTING PERFORMANCE STUDY

6.1 Scenario Description

A study is conducted to evaluate dim star pointing performance. Dim stars are defined as having visual magnitudes in the range from 13 to 20. The fast scale has sampling period $t_\Delta = .002$ seconds. The slow scale has a sampling period corresponding to the camera exposure time T seconds, which takes different values depending on star magnitude and type. Latencies are defined as $\ell = m = 0.006$ sec, and modeled using 3'rd order Pade appxomations.

6.1.1 Plant

The plant consists of a fast-steering mirror with an inner loop wrapped around it having a bandwidth of 125 Hz, so that its function is nearly unity (i.e., $P(s) \simeq 1$) over low frequencies. This simplifies the digital controller design.

6.1.2 Control Design

A deadbeat controller is used that brings the target directly to the desired position in a single sampling period. For a unity-gain plant (neglecting delays), a deadbeat controller is given by a simple unity gain integrator,

$$C(z) = \frac{1}{z-1} \tag{6.1}$$

Using controller (6.1) in closed-loop with a unity-gain plant, the response to a constant reference r is tracked in a single time step, and the response to a constant load disturbance is rejected in a single step. The deadbeat controller (6.1) is ideal for pointing at dim stars where the exposure times T are long compared to the 125 Hz plant response (i.e., 1/125=.008 seconds). This includes all of the cases to be considered in the current paper, for which the smallest T is 8 seconds. For brighter stars, however, the controller is gain-scheduled as a function of T.[2]

6.1.3 Noncommon Thermal Errors

Noncommon thermal errors are modeled using a coloring filter derived from a PSD specification.[2]

6.1.4 Centroiding Errors

SIM centroiding error $\sigma_c(T)$ is analyzed in Alexander.[1] Analysis indicates that $\sigma_c(T)$ depends on the location on the pixel where the centroid is taken. In particular, a natural "crosshair" is formed at the intersection of any four neighboring pixels. If the centroid is within 10 percent of this crosshair, centroids are generally improved. This effect is taken into account in the current study.

6.1.5 Fixed Errors

The fixed error term σ^2_{fixed} is comprised of four components: (1) RWA-induced jitter (20 mas) (2) FSM quantization/mechanical errors (7.1 mas), (3) pointing calibration error (11.3 mas), and (4) error in the feedforward signal (20 mas). These errors RSS to a value of $\sigma_{fixed} = 31$ mas (1-sigma, radial).

6.2 Family of Optimal Designs

A family of optimal pointing designs for SIM is given in this section parametric on star magnitudes and centroided pixel location. Similar studies are given in Bayard and Kang[2] parametric on star type. Optimal pointing results are shown in Figure 6.1 for an A-type star centroided at a pixel center, and in Figure 6.2 for an A-type star centroided at a pixel crosshair. Here, a fixed error of 31 mas (1-sigma, radial) has been RSS'ed with the noncommon thermal error to define the single black curve. In the plots, the single black curve is shown RSS'ed with various colored curves corresponding to the centroiding error for different star magnitudes, to form the total error curve (dashed). The total error curve is plotted as a thick dashed line that is colored-coded to match the corresponding centroiding error curve from which it was calculated.

Numerical results indicate that a centroid measurement taken at a pixel crosshair gives an improvement in pointing performance worth approximately 1 magnitude in star brightness compared to a centroid taken at some arbitrary location on the pixel. For example, pointing performance for the magnitude 19 star in plot Figure 6.1 (blue) is comparable to the magnitude 20 star in plot Figure 6.2 (purple).

7. CONCLUSIONS

The PCAT tool has been developed for general purpose covariance analysis of pointing control systems. PCAT-S represents the specialization of PCAT to the SIM science pointing subsystem.

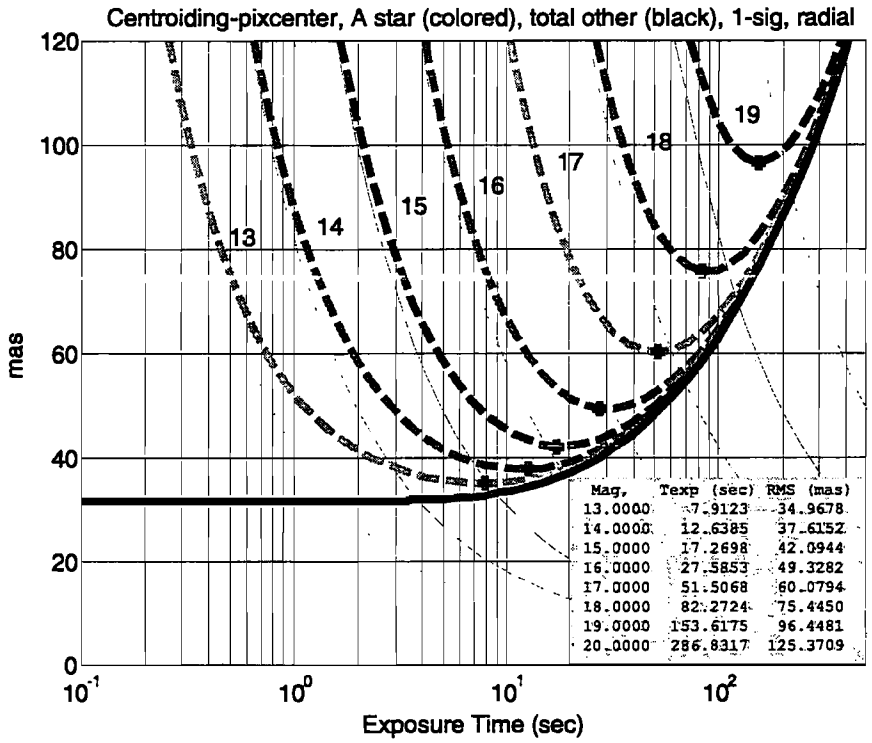

Figure 6.1. Family of optimal designs parametric on star magnitude. Assumes an A-type star centroiding at *pixel center*, 1-sigma, radial, mas.

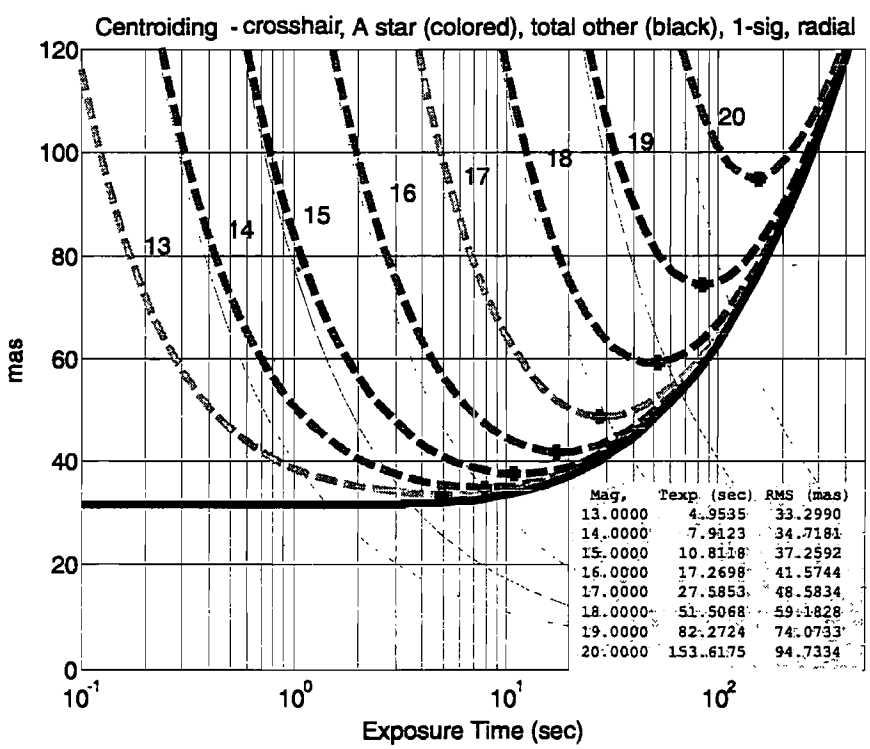

Figure 6.2. Family of optimal designs parametric on star magnitude. Assumes an A-type star centroiding at *pixel crosshair*, 1-sigma, radial, mas.

The PCAT-S tool has been applied to analyzing the challenging problem of dim-star pointing for stars in the visual magnitude range from 13 to 20. Results are summarized in Figure 6.1, Figure 6.2. Results indicate that pointing performance can be optimized by choosing exposure times as a function of the magnitude and type of star being pointed at, and where on the pixel the star is centroided. As expected, pointing performance is best when pointing at brighter stars and worse for dimmer stars. Also, best performance is obtained when the star is centroided near a pixel crosshair rather than some other arbitrary location on the pixel.

The results of this paper do not support earlier more optimistic dim-star pointing performance predictions, made based on less detailed analysis. Because the current designs are optimal, they place a fundamental limit on what is attainable in practice. For example, the designs shown in Figure 6.1 are optimized for an A-type star centroided at a pixel center, and indicate that as the star brightness degrades from magnitude 13 to 19, the optimal exposure times increase from 8 to 300 seconds, and the associated pointing performance degrades from 35 to 125 mas (1-sigma radial).

In simple terms, the optimal exposure times can be interpreted as trading off the contribution of centroiding error with thermomechanical drift error. Centroiding errors increase with short exposures (less signal), while thermomechanical drift errors increase with long exposures (more time to drift). The result is an optimal exposure time lying somewhere in-between that balances these two opposite effects. Methods to improve performance include making the telescope aperture larger to accept more photons (reduced centroiding error), or to make the structure more stable with respect to thermal variations (less thermomechanical drift). The PCAT-S studies indicate that if centroiding errors are reduced, the optimal designs will favor shorter exposure times, while if thermal drift is reduced, the optimal designs will favor longer exposure times. Interestingly, reducing RWA induced jitter beyond its current 20 mas level will have little effect on improving pointing performance for stars dimmer than magnitude 15, since in this range pointing errors are dominated by the centroiding and thermal drift components.

An unanticipated result from the performance analysis indicates that a centroid measurement taken at a pixel crosshair gives an improvement in pointing performance worth approximately 1 magnitude in star brightness compared to a centroid taken at some arbitrary location on the pixel. This motivates designing a system, if possible, that takes all centroids in close proximity to a pixel crosshair.

As stars become brighter, optimal exposure times become shorter and at some point there will be an additional benefit to smoothing centroid measurements over multiple samples. This extra smoothing is not captured in the present paper, and hence performance limits presented here should not be extrapolated to bright star pointing without a separate analysis.

ACKNOWLEDGMENTS

This work was performed at the Jet Propulsion Laboratory under contract with the National Aeronautics and Space Administration.

REFERENCES

1. J. Alexander, "RTC reference stars and throughput model user's guide," JPL Internal Document, November 7, 2006.
2. D.S. Bayard and B.H. Kang, "SIM instrument pointing control performance analysis," JPL Internal Document, JPL D-37846, July 23, 2007.
3. A. Gelb (Ed.), *Applied Optimal Estimation.* The MIT Press, Cambridge, Massachusetts, 1984.
4. B.H. Kang, D.S. Bayard and Glenn Macala, "SIM-Planet Quest interferometer real-time control system architecture," SPIE Optics & Photonics 07, San Diego, CA, August 26-30, 2007.
5. R.A. Laskin, "Space Interferometer Mission (SIM) - technology completion and transition to flight," in *Proc. SPIE Conference on Astronomical Telescopes and Instrumentation*, Glasgow, Scotland United Kingdom, June 21-25, 2004, SPIE 5491-37.
6. J.C. Marr, "Space Interferometry Mission (SIM): Overview and current status," in *Proc. SPIE* Vol. 4852, pp. 1-15, Interferometry in Space; Michael Shao (Ed.), February 2003.
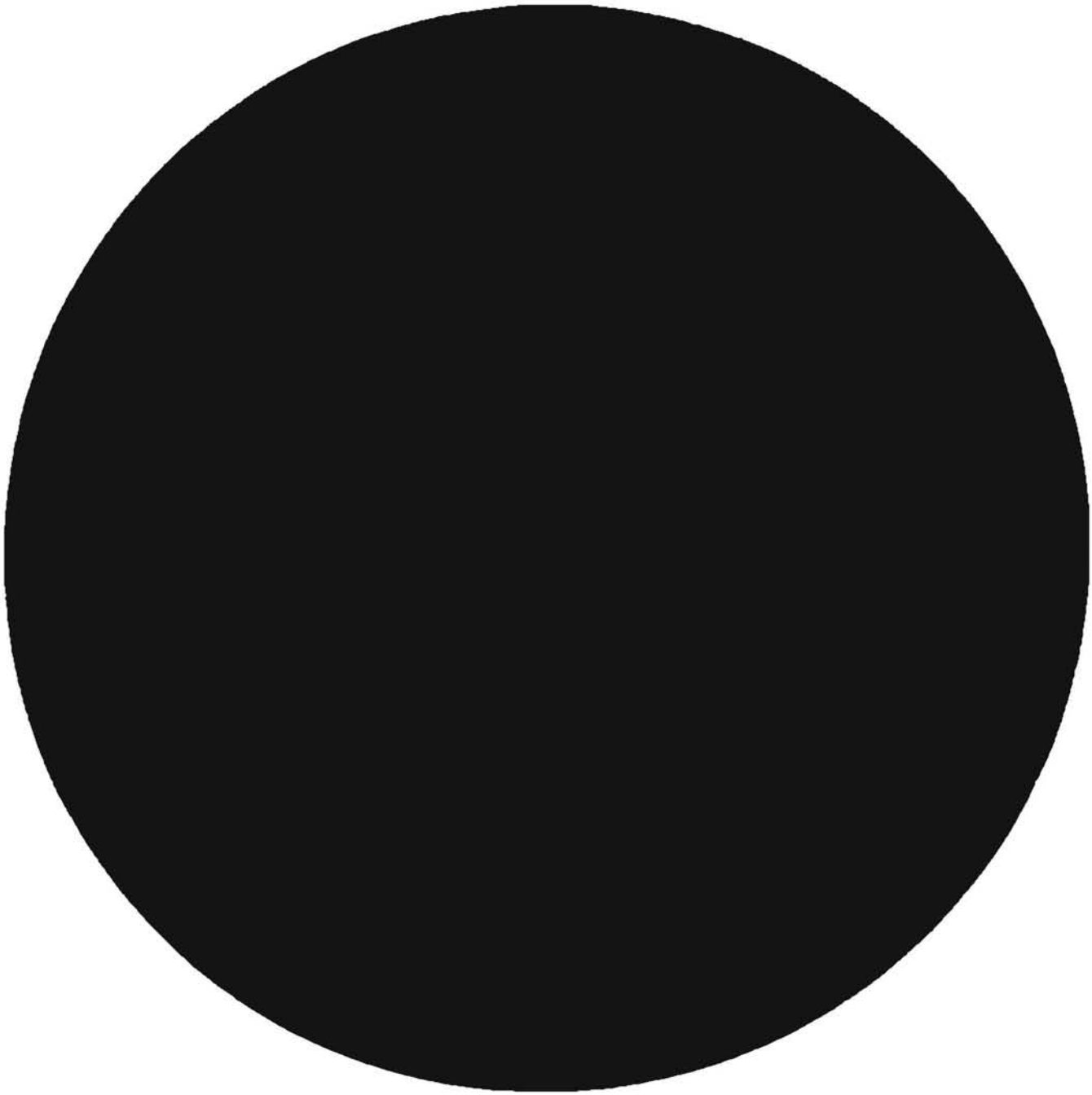
End of File